Acta Crystallographica Section F
Structural Biology and Crystallization Communications
ISSN 1744-3091

A preliminary crystallographic study of recombinant NicX, an Fe^{2+}-dependent 2,5-dihydroxypyridine dioxygenase from *Pseudomonas putida* KT2440

José Ignacio Jiménez,[a]‡§ Iván Acebrón,[b]§ José Luis García,[a] Eduardo Díaz[a] and José Miguel Mancheño[b]*

[a]Departamento de Biología Medioambiental, Centro de Investigaciones Biológicas, CSIC, Ramiro de Maeztu 9, 28040 Madrid, Spain, and [b]Grupo de Cristalografía Macromolecular y Biología Estructural, Instituto de Química Física Rocasolano, CSIC, Serrano 119, 28006 Madrid, Spain

‡ Present address: FAS Center for Systems Biology, Northwest Building, 52 Oxford Street, Cambridge, Massachusetts, USA.
§ These authors contributed equally to this work.

Correspondence e-mail: xjosemi@iqfr.csic.es

Received 24 February 2010
Accepted 24 March 2010

NicX from *Pseudomonas putida* KT2440 is an Fe^{2+}-dependent dioxygenase that is involved in the aerobic degradation of nicotinic acid. The enzyme converts 2,5-dihydroxypyridine to *N*-formylmaleamic acid when overexpressed in *Escherichia coli*. Biophysical characterization of NicX by analytical gel-filtration chromatography revealed that it behaves as an oligomeric assembly in solution, with an apparent molecular weight that is consistent with a hexameric species. NicX was crystallized by the hanging-drop vapour-diffusion method at 291 K. Diffraction data were collected to a resolution of 2.0 Å at the ESRF. The crystals most probably belong to the orthorhombic space group *C*222 or $C222_1$. The estimated Matthews coefficient was 2.4 $Å^3$ Da^{-1}, corresponding to 50% solvent content, which is consistent with the presence of three protein molecules in the asymmetric unit. Analysis of the crystal data together with chromatographic results supports NicX being a hexameric assembly composed of two cyclic trimers. Currently, crystallization of recombinant selenomethionine-containing NicX is in progress.

1. Introduction

Dioxygenases catalyze the incorporation of the two atoms of molecular oxygen into a broad range of compounds, leading to the oxidative cleavage of carbon–carbon bonds and monohydroxylation and dihydroxylation reactions (Bugg & Ramaswamy, 2008). The subgroup of nonhaem iron-dependent dioxygenases act on both single-ring and multi-ring aromatic compounds and play an important role in their aerobic metabolism (Lipscomb, 2008). As a consequence of their activity, chemically stable aromatic compounds are transformed into aliphatic intermediates owing to the cleavage of their aromatic rings. In turn, these metabolites are used as the nutrition source for microorganisms *via* the citric acid cycle (Harwood & Parales, 1996). According to their mode of ring cleavage, the ring-cleaving oxygenases are classified as intradiol and extradiol dioxygenases, which are both structurally and functionally distinct (Bugg, 2003; Vaillancourt *et al.*, 2006). For instance, whereas intradiol dioxygenases utilize Fe^{3+} as a cofactor, which is ligated by two tyrosine ligands and two histidine ligands, extradiol dioxygenases utilize Fe^{2+}, which is ligated by two histidine ligands and a glutamic acid ligand (Bugg & Ramaswamy, 2008). The arrangement of the latter metal ligands, which is known as the 2-His-1-carboxylate facial triad motif (Koehntop *et al.*, 2005), is present in over 20 families of enzymes and exhibits remarkable catalytic versatility (Lipscomb, 2008).

NicX from *Pseudomonas putida* KT2440 is an Fe^{2+}-dependent extradiol dioxygenase that converts 2,5-dihydroxypyridine (2,5-DHP) to *N*-formylmaleamic acid (NFM; Fig. 1), which constitutes the third step in the aerobic nicotinic acid (NA) degradation pathway (Jiménez *et al.*, 2008). Living cells contain NA (niacin, vitamin B_3) in the form of pyridine cofactors (NAD and NADP) at concentrations of 0.1–1 m*M* (London & Knight, 1966) and NA is also a carbon, nitrogen and energy source for a diverse set of organisms (Fetzner, 1998). Despite the pharmacological and agrochemical value of the bio-

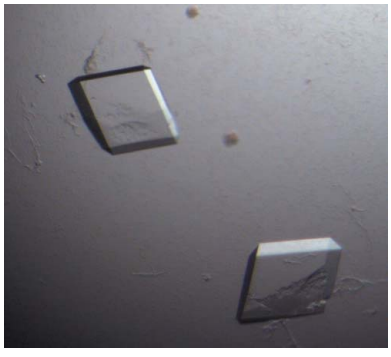

chemical pathways involved in the degradation of NA (Yoshida & Nagasawa, 2000), only two catabolic pathways have been fully elucidated to date, namely the anaerobic route from *Eubacterium barkeri* (Alhapel *et al.*, 2006) and the aerobic route from *P. putida* KT2440 (Jiménez *et al.*, 2008). *E. barkeri* metabolizes NA to propionate and pyruvate in nine steps, yielding a single ATP per nicotinate (Alhapel *et al.*, 2006). To date, four enzymes that participate in this route have been structurally characterized: nicotinate dehydrogenase (PDB code 3hrd; Wagener *et al.*, 2009), enamidase (PDB code 2vun; Kress *et al.*, 2008), 2-(hydroxymethyl)glutarate dehydrogenase (PDB code 3cky; Reitz *et al.*, 2008) and (*R*)-3-methylaconitate-Δ-isomerase (PDB code 3g7k; Velarde *et al.*, 2009). Conversely, *P. putida* metabolizes NA to fumarate in six steps (Jiménez *et al.*, 2008) and, in contrast to the above case, no enzyme from this route has been structurally characterized. With the aim of shedding light on the structural basis of the aerobic metabolism of NA in *P. putida*, we have focused our attention on NicX, a novel Fe^{2+}-dependent dioxygenase which according to sequence analysis defines a new family of extradiol dioxygenases (Jiménez *et al.*, 2008).

In this work, we have crystallized recombinant NicX produced in *Escherichia coli* and also provide preliminary X-ray crystallographic analysis.

2. Experimental methods

2.1. Protein expression and purification

The pETNicX plasmid overexpressing the *nicX* gene under the control of the P_{T7} promoter and *lac* operator was constructed by cloning the 1.1 kb *Nde*I/*Eco*RI PCR-amplified *nicX* gene into the expression vector pET-29a(+) (Novagen; Jiménez *et al.*, 2008). The NicX protein was overproduced in *E. coli* BL21 (DE3) cells carrying the recombinant plasmid pETNicX (Jiménez *et al.*, 2008). The cells were grown at 303 K in LB medium with kanamycin (50 µg ml^{-1}) until they reached an optical density at 600 nm of ∼0.6. Protein expression was induced by the addition of isopropyl β-D-1-thiogalactopyranoside (IPTG; 1 m*M* final concentration). After induction, the cells were grown at 303 K for 12 h and collected by centrifugation.

The purification of recombinant NicX was accomplished as follows. The bacterial cell pellet was resuspended in 50 m*M* NaH_2PO_4 pH 7.5 buffer (10 ml buffer per 200 ml cell culture) and homogenized using a French press. The lysate was centrifuged in an SS34 rotor at 15 000 rev min^{-1} using a Sorvall centrifuge for 15 min at 277 K to remove the cell debris. The clear supernatant was then applied onto a DEAE-cellulose column previously equilibrated with 50 m*M* NaH_2PO_4 pH 7.5 buffer. The column was washed with 20 volumes of phosphate buffer containing 0.1 *M* NaCl. NicX was purified in a linear gradient of NaCl (0.1–0.3 *M*) in 20 m*M* NaH_2PO_4 pH 7.5. Fractions showing 2,5-DHP dioxygenase activity were pooled and dialyzed against 20 m*M* NaH_2PO_4 pH 7.5. The protein was further purified by hydroxyapatite chromatography using a linear gradient (20–100 m*M*) of NaH_2PO_4 pH 7.0. Fractions showing 2,5-DHP dioxygenase activity were pooled and dialyzed against 20 m*M* NaH_2PO_4 pH 7.5. The purified recombinant material thus obtained was concentrated to 9–10 mg ml^{-1} using YM-10 Centricon filters (Millipore). Buffer-exchange to 20 m*M* HEPES pH 7.5 with 0.1 *M* NaCl and 2 m*M* DTT for crystallization trials (see below) was carried out using a HiTrap desalting column (GE Healthcare) on an ÄKTA-prime system (Pharmacia). Protein concentration was determined by UV–Vis absorbance measurements with a Nanodrop ND-1000 spectrophotometer using an extinction coefficient of 1.15 (1 mg ml^{-1}, 1 cm, 280 nm) as estimated using the *ExPASy* sever (Gasteiger *et al.*, 2005). The overall yield was 15 mg pure NicX per litre of culture. SDS–PAGE gels were run and stained with Coomassie blue at each step of purification to estimate the protein purity and abundance.

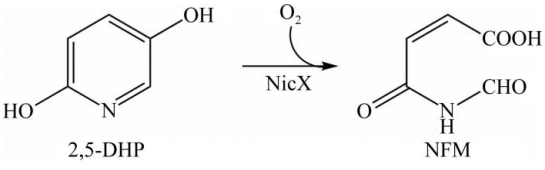

Figure 1
Reaction scheme showing the NicX-catalyzed conversion between 2,5-dihydroxypyridine (2,5-DHP) and *N*-formylmaleamic acid (NFM).

Purified NicX was enzymatically active, as assayed under standard assay conditions in the presence of exogenous Fe^{2+}, and maintained its activity when stored at 277 K in 20 m*M* HEPES pH 7.5, 0.1 *M* NaCl and 2 m*M* DTT for several days.

2.2. Enzyme assay

The 2,5-DHP dioxygenase activity of purified NicX was determined spectrophotometrically by monitoring the time-dependence of the 2,5-DHP absorbance change at 320 nm (ε = 5200 M^{-1} cm^{-1}) as described previously (Gauthier & Rittenberg, 1971). Prior to activity measurements, NicX (5 µg; 50 µl total volume) was preincubated (reactivation) at 298 K for 15 min in the presence of 20 m*M* NaH_2PO_4 pH 7.5, 8 m*M* DTT and 420 µ*M* ferrous sulfate in a total volume of 120 µl. The reaction mixture was then diluted with 20 m*M* NaH_2PO_4 pH 8.0 (1 ml total volume). In our standard assay conditions, 13.6 µl 10 m*M* 2,5-DPH (200 µ*M* final concentration in the reaction mixture) was added to 680 µl of the latter NicX solution and the absorbance of 2,5-DHP was continuously monitored at 298 K in a Beckman DU-520 spectrophotometer.

2.3. Analytical size-exclusion chromatography

Analytical size-exclusion chromatography was performed on a Superdex 200 10/300 GL Tricorn column (GE Healthcare) equilibrated with 20 m*M* HEPES pH 7.5, 0.1 *M* NaCl and 2 m*M* DTT. The column was calibrated using thyroglobulin (667 kDa), apoferritin (443 kDa), β-amylase (200 kDa), alcohol dehydrogenase (150 kDa), bovine serum albumin (66 kDa), ovalbumin (45 kDa), carbonic anhydrase (29 kDa), sperm whale myoglobin (17 kDa) and vitamin B_{12} (1.3 kDa) in the same buffer. The size of NicX was determined from its K_{av} value [$K_{av} = (V_e - V_0)/(V_t - V_0)$, where V_e is the elution volume, V_0 is the void volume and V_t is the total volume of the column] by interpolation in a calibration semi-log plot of the molecular mass of the standard proteins *versus* their K_{av} values.

2.4. Mass spectrometry and N-terminal sequencing

Matrix-assisted laser desorption/ionization time-of-flight mass spectrometry (MALDI–TOF MS) on a Finnigan LCQ Deca ion-trap mass spectrometer (Thermo Electron, San José, California, USA) was used to determine the molecular mass of NicX. Mass spectra were recorded in full scan mode (m/z = 450–2000) and the protein peaks detected were deconvoluted using the *BIOMASS* deconvolution tool from the *BioWorks* 3.1 software (Thermo Fisher Scientific). The N-terminal automated sequence analysis of pure NicX was carried out using an Applied Biosystems model 477A protein sequencer.

2.5. Crystallization

Initial crystallization conditions for NicX at 291 K were determined by the sparse-matrix method (Jancarik & Kim, 1991) with commercial screens from Hampton Research (Riverside, California, USA) in crystallization trials using the sitting-drop vapour-diffusion method in Innovaplate SD-2 96-well plates. Small crystals of NicX appeared in 30%(*w*/*v*) PEG 4000, 0.2 *M* sodium acetate trihydrate, 0.1 *M* Tris–HCl pH 8.5. Optimization of the crystallization conditions using JBScreens 2 and 3 from Jena Bioscience rendered crystals in 22%(*w*/*v*) PEG 4000, 0.1 *M* sodium acetate and 0.1 *M* HEPES pH 7.5 and also in 20%(*w*/*v*) PEG 4000, 0.2 *M* lithium sulfate and 0.1 *M* Tris–HCl pH 8.5. The final optimized crystallization conditions determined with the use of Additive Screen from Hampton Research (Riverside, California, USA) produced crystals that diffracted with high quality in hanging drops containing 1 µl protein solution (14 mg ml^{-1} in 20 m*M* HEPES pH 7.5 with 0.1 *M* NaCl and 2 m*M* DTT), 1 µl reservoir solution [22%(*w*/*v*) PEG 4000, 0.1 *M* sodium acetate and 0.1 *M* HEPES pH 7.5 with 2 m*M* DTT] and 1 µl 50 m*M* EDTA.

2.6. Data collection and reduction

Crystals for X-ray analysis were transferred to an optimized cryoprotectant solution [reservoir solution plus 15%(*v*/*v*) glycerol] for ∼5 s and were then cryocooled at 100 K in a cold nitrogen-gas stream. Diffraction data were recorded using an ADSC Q210 CCD detector (Area Detector Systems Corporation) on beamline ID23-1 at the European Synchrotron Radiation Facility (ESRF; Grenoble, France). The images were processed and scaled using *MOSFLM* (Leslie, 1999) and *SCALA* from the *CCP*4 program suite (Collaborative Computational Project, Number 4, 1994). Intensities were converted to structure-factor amplitudes using *TRUNCATE* (Collaborative Computational Project, Number 4, 1994). The self-rotation function was calculated with the *CCP*4 program *MOLREP* (Vagin & Teplyakov, 1997).

3. Results and discussion

2,5-Dihydroxypyridine dioxygenase (NicX) from *P. putida* KT2440 lacking any additional tag was overproduced from *E. coli* BL21 (DE3) cells carrying the recombinant plasmid pETNicX (Jiménez *et al.*, 2008) as described in §2. Cell extracts were used to detect the presence of hyperproduced proteins by SDS–PAGE analysis. The expression of an additional 39 kDa protein was apparent in cells harbouring pETNicX upon induction with 1 m*M* IPTG at an OD_{600} of ∼0.6. The expression levels were highest ∼12 h after induction at 303 K. Higher concentrations of IPTG or incubation at 310 K led to a higher proportion of insoluble material. Conversely, lower concentrations of IPTG or lower temperatures led to a decreased initial yield of the enzyme.

The optimal yield and highest specific activity were obtained by following the purification protocol described in §2. The final yield of soluble NicX was estimated to be approximately 15 mg per 1000 ml of liquid culture.

The molecular mass of monomeric NicX was determined by MALDI–TOF MS analysis. A mass value of m/z = 38 883.0 was observed, which compares well with the calculated average mass of 38 886.1 Da for recombinant NicX without the amino-terminal Met residue (349 amino-acid residues). This result agrees with N-terminal automated sequence analysis carried out using an Applied Biosystems model 477A protein sequencer, which provided the sequence PVSNAQLT, which was in perfect agreement with the sequence deduced from the nucleotide sequence of the *nicX* gene (PP3945).

The oligomeric state of NicX (250 µ*M*) in solution was studied by analytical gel-filtration chromatography on a Superdex 200 10/300 GL Tricorn column in conjunction with SDS–PAGE. The results obtained indicated that NicX exists in solution as a species of 243.2 ± 4.3 kDa (n = 3; Fig. 2), with subunits of ∼39 kDa. These results compare well with the theoretical mass expected for hexameric NicX (233.3 kDa). Taken together, these results indicated that (at 250 µ*M*) NicX behaves in solution as a homogeneous hexameric species, which is also in agreement with the oligomeric state previously reported for 2,5-DHP dioxygenase from *P. putida* N-9 (Gauthier & Rittenberg, 1971).

The initial crystals of NicX obtained in crystallization trials using the sitting-drop vapour-diffusion method grew as small plates in 30%(*w*/*v*) PEG 4000, 0.2 *M* sodium acetate trihydrate, 0.1 *M* Tris–HCl pH 8.5. Screens based on PEG 4000 as a precipitant from Jena Bioscience (JBScreens 2 and 3) produced crystals in 22%(*w*/*v*) PEG 4000, 0.1 *M* sodium acetate and 0.1 *M* HEPES pH 7.5 and also in 20%(*w*/*v*) PEG 4000, 0.2 *M* lithium sulfate and 0.1 *M* Tris–HCl pH 8.5.

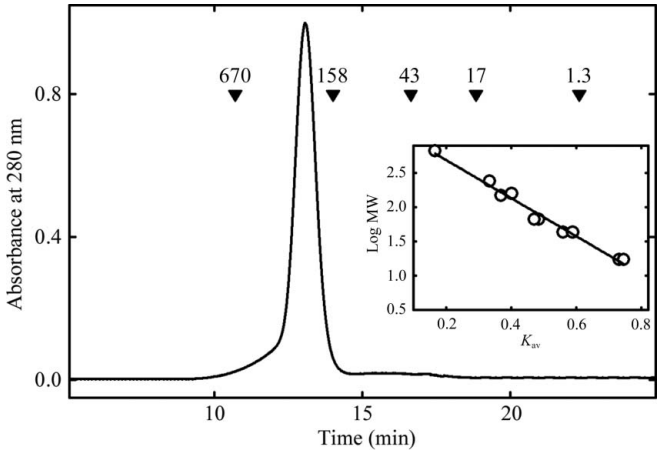

Figure 2
Analytical gel-filtration studies of NicX. The elution profile of NicX is shown together with the elution positions of standard proteins. The scale at the bottom indicates the elution time. Inset: semi-log plot of the molecular mass of the standard proteins used *versus* their K_{av} values.

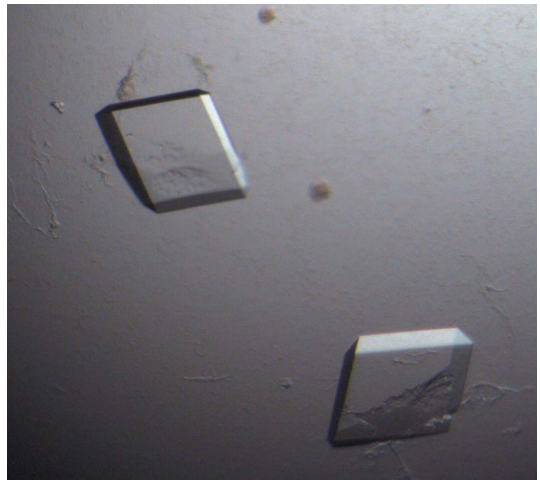

Figure 3
Optimized crystals of recombinant NicX from *P. putida* KT2440 grown at 291 K in 22%(*w*/*v*) PEG 4000, 0.1 *M* sodium acetate and 0.1 *M* HEPES pH 7.5 with 2 m*M* DTT. The final drops contained 1 µl protein solution (14 mg ml^{-1} in 20 m*M* HEPES pH 7.5 with 0.1 *M* NaCl and 2 m*M* DTT), 1 µl reservoir solution and 1 µl 50 m*M* EDTA.

Optimized crystallization conditions were determined using Additive Screen from Hampton Research (Riverside, California, USA). Finally, large prism-shaped crystals (0.1 × 0.3 × 0.5 mm) that diffracted with high quality were obtained in hanging drops containing 1 µl protein solution (14 mg ml^{-1} in 20 m*M* HEPES pH 7.5 with 0.1 *M* NaCl and 2 m*M* DTT), 1 µl reservoir solution [22%(*w*/*v*) PEG 4000, 0.1 *M* sodium acetate and 0.1 *M* HEPES pH 7.5 with 2 m*M* DTT] and 1 µl 50 m*M* EDTA (Fig. 3). The collected data set was 80.8% complete to 2.00 Å resolution and merged with an overall $R_{\rm merge}$ of 12.0%. Data-collection statistics are given in Table 1. The crystals most probably belong to the orthorhombic space group *C*222 or *C*222$_1$, with unit-cell parameters a = 107.2, b = 139.5, c = 142.8 Å. The number of molecules in the crystallographic asymmetric unit was estimated using the Matthews probability calculator (Kantardjieff & Rupp, 2003). The highest probability (0.83) was observed for three molecules in the asymmetric unit, giving a Matthews coefficient ($V_{\rm M}$; Matthews, 1968) and solvent content of 2.4 Å^3 Da^{-1} and 49.8%, respectively. Analysis of the self-rotation function (Fig. 4*a*) calculated from the crystal data using *MOLREP* from the *CCP*4 suite shows features at χ = 180° indicating the 222 point-group symmetry of the NicX crystal and also the presence of a local threefold axis at (θ, φ, χ) = (80, 90, 120°) (Fig. 4*b*). The presence of the local threefold axis probably arises from a cyclic arrangement of the three independent NicX molecules making up the asymmetric unit. These results, together with those from analytical gel-filtration chromatography, provide experimental evidence supporting the idea that NicX is an oligomeric assembly composed of cyclic trimers. The preparation of crystals of selenomethionine-containing NicX for structure solution by MAD is currently in progress.

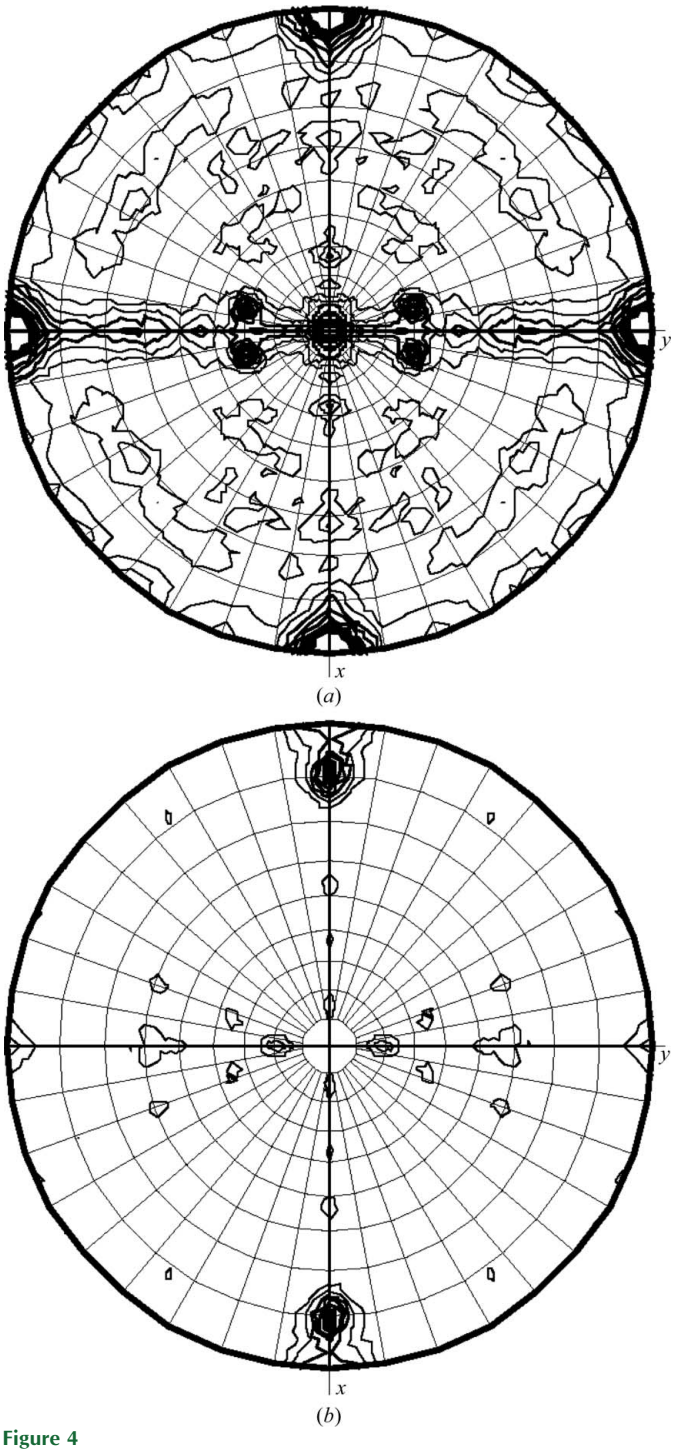

Figure 4
Self-rotation functions. (*a*) κ = 180° section of the self-rotation function calculated from the NicX crystal. (*b*) κ = 120° section showing prominent nontrivial peaks. All calculations were performed with *MOLREP* (Vagin & Teplyakov, 1997) based on data from 30.0 to 3.5 Å resolution with a radius of integration of 25 Å. The labelling of the x and y axes is according to the orthogonal coordinate system defined by *MOLREP*.

Table 1
Data-collection and processing statistics.

Values in parentheses are for the highest resolution shell.

Beamline	ID23-1, ESRF
Wavelength (Å)	1.0675
Space group	*C*222 or *C*222$_1$
Unit-cell parameters (Å)	a = 107.2, b = 139.5, c = 142.8
$V_{\rm M}$ (Å^3 Da^{-1})	2.4
Monomers per ASU	3
Solvent content (%)	49.8
Resolution range (Å)	85.12–2.00 (2.11–2.00)
$R_{\rm merge}$ (%)	12.0 (45.5)
Mean $I/\sigma(I)$	11.2 (3.2)
No. of measured reflections	343777
No. of unique reflections	58196 (7977)
Completeness (%)	80.8 (80.8)
Multiplicity	5.9 (5.9)

JMM thanks the Ministerio de Educación y Ciencia for a research grant (BFU2007-67404/BMC), 'Factoría de Cristalización' Consolider-Ingenio 2010 for support of his research and the ESRF (Grenoble, France) for provision of synchrotron-radiation facilities. ED and JLG acknowledge the Ministerio de Ciencia e Innovación for grants GEN2006-27750-C5-3-E, BIO2006-05957 and CSD2007-00005 and the Comunidad Autónoma de Madrid for grant P-AMB-259-0505. IA is the recipient of an FPU predoctoral fellowship from the Ministerio de Educación. JIJ was the recipient of an I3P predoctoral fellowship from the Consejo Superior de Investigaciones Científicas.

References

Alhapel, A., Darley, D. J., Wagener, N., Eckel, E., Elsner, N. & Pierik, A. J. (2006). *Proc. Natl Acad. Sci. USA*, **103**, 12341–12346.
Bugg, T. D. H. (2003). *Tetrahedron*, **59**, 7075–7101.
Bugg, T. D. H. & Ramaswamy, S. (2008). *Curr. Opin. Chem. Biol.* **12**, 134–140.
Collaborative Computational Project, Number 4 (1994). *Acta Cryst.* D**50**, 760–763.
Fetzner, S. (1998). *Appl. Microbiol. Biotechnol.* **49**, 237–250.
Gasteiger, E., Hoogland, C., Gattiker, A., Duvaud, S., Wilkins, M. R., Appel, R. D. & Bairoch, A. (2005). *The Proteomics Protocols Handbook*, edited by J. M. Walker, pp. 571–608. Totowa: Humana Press.
Gauthier, J. J. & Rittenberg, S. C. (1971). *J. Biol. Chem.* **246**, 3737–3742.

Harwood, C. S. & Parales, R. E. (1996). *Annu. Rev. Microbiol.* **50**, 553–590.
Jancarik, J. & Kim, S.-H. (1991). *J. Appl. Cryst.* **24**, 409–411.
Jiménez, J. I., Canales, A., Jiménez-Barbero, J., Ginalski, K., Rychlewski, L., García, J. L. & Díaz, E. (2008). *Proc. Natl Acad. Sci. USA*, **105**, 11329–11334.
Kantardjieff, K. A. & Rupp, B. (2003). *Protein Sci.* **12**, 1865–1871.
Koehntop, K. D., Emerson, J. P. & Que, L. Jr (2005). *J. Biol. Inorg. Chem.* **10**, 87–93.
Kress, D., Alhapel, A., Pierik, A. J. & Essen, L.-O. (2008). *J. Mol. Biol.* **384**, 837–847.
Leslie, A. G. W. (1999). *Acta Cryst.* D**55**, 1696–1702.
Lipscomb, J. D. (2008). *Curr. Opin. Struct. Biol.* **18**, 644–649.
London, J. & Knight, M. (1966). *J. Gen. Microbiol.* **44**, 241–254.
Matthews, B. W. (1968). *J. Mol. Biol.* **33**, 491–497.
Reitz, S., Alhapel, A., Essen, L.-O. & Pierik, A. J. (2008). *J. Mol. Biol.* **382**, 802–811.
Vagin, A. & Teplyakov, A. (1997). *J. Appl. Cryst.* **30**, 1022–1025.
Vaillancourt, F. H., Bolin, J. T. & Eltis, L. D. (2006). *Crit. Rev. Biochem. Mol. Biol.* **41**, 241–267.
Velarde, M., Macieira, S., Hilberg, M., Bröker, G., Tu, S.-M., Golding, B. T., Pierik, A. J., Buckel, W. & Messerschmidt, A. (2009). *J. Mol. Biol.* **391**, 609–620.
Wagener, N., Pierik, A. J., Ibdah, A., Hille, R. & Dobbek, H. (2009). *Proc. Natl Acad. Sci. USA*, **106**, 11055–11060.
Yoshida, T. & Nagasawa, T. (2000). *J. Biosci. Bioeng.* **89**, 111–118.